

Measurement of Neutron Electric Dipole Moment

Y. Arimoto, K. Asahi, H. Fujioka, H. Funahashi, M. Hino, T. Ino,
H. Iwase, Y. Iwashita, Y. Kamiya, T. Kawai, N. Kimura, M. Kitaguchi,
Y. Kiyanagi, S. Komamiya, K. Mishima, S. Muto, T. Ogitsu, K. Sakai,
T. Shima, H. M. Shimizu, K. Taketani, M. Utsuro, S. Yamashita,
A. Yoshimi, and T. Yoshioka

(NOP Collaboration)

1 Executive Summary

We propose to measure the electric dipole moment (EDM) of ultracold neutrons (UCNs) with the experimental sensitivity of 6×10^{-28} e-cm by constructing a UCN source driven by the pulsed proton beam at J-PARC. The sensitivity can be achieved by suppressing the systematic errors using downsized UCN storage volume. In order to improve the statistics in the smaller volume, we improve a time-focusing optics to transfer the instantaneously dense UCN, which can be obtained at a short-pulse spallation neutron source, to a remote place without losing the density. The proton beam of the J-PARC is almost ideal for this strategy. Please refer to the summary of the J-PARC UCN Taskforce [1] in which the availability of the proton beam and the candidates of the location were discussed in 2009.

2 Introduction

Attempts to measure the electric dipole moment (EDM) of neutrons have played an important role in the search for the new physics beyond the standard model of the elementary particles.

Discovery of a non-zero value of the EDM unambiguously signals the breaking of the time reversal invariance, which leads to a significant progress. The breaking of time reversal invariance is equivalent to the breaking of the CP symmetry assuming the CPT invariance in quantum field theory. The CP-violating phase in the CKM matrix is insufficient to explain the baryon asymmetry in the universe. The value of the EDM of atoms, electrons and nuclei has been searched for identifying additional source or sources of the CP-violation.

The advantages of the EDM measurement in the search for new physics are following.

1. the standard model delivers extremely small values ($d_n \sim 10^{-32}$ e-cm),

2. new physics beyond the standard model, such as the supersymmetric model (SUSY) or multi-Higgs model, naturally predict large values of EDM in orders of magnitudes,
3. present experimental sensitivities are reaching to those theoretical predictions and the value of EDM delivered by the new physics is expected to be experimentally discovered by improving the experimental sensitivity by one or two orders of magnitudes.

The EDM and the lepton flavor violation (LFV) are the most promising phenomena, in which the experimental sensitivity is very close to the predictions of theoretical models beyond the standard model.

The neutron EDM can be interpreted directly with the down quark EDM.

$$d_n \simeq 1.1 \times e(0.5d_u^c + d_d^c) + 1.4 \times (-0.25d_u + d_d) \quad (1)$$

It can be related with the electron EDM through the grand unified theory (GUT) to bridge the quark and lepton sectors. The relation depends on the theoretical models, thus the neutron EDM and electron EDM gives us the complementary information on the new physics.

A new physics is expected in the TeV scale to avoid the unnatural fine-tuning, that is, the hierarchy problem of the standard model. The possibility is suggested from the coincidence of coupling constants at the GUT scale in the extrapolation of experimental data obtained at the high energy frontier (e.g. LEP) based on the SUSY-GUT model, the new framework such as the see-saw mechanism to explain the neutrino mass delivered from the Super-KAMIOKANDE. It leads to the expectation of the direct observation of Higgs bosons and SUSY particles in the LHC experiments, which is being initiated in Europe.

A large value of the neutron EDM can be predicted in many theoretical models. If we allow to introduce the imaginary phase among newly introduced particles carrying color charges in the same manner as the CKM matrix, some of the observables can easily exceed the existing experimental upper bounds. The structure of the scalar quark sector in the SUSY is strongly constrained by those experimental upper bounds especially by the neutron EDM upper bound. Indeed, while the structure of the minimal supersymmetric standard model (MSSM) is most strongly constrained by the result of the Higgs search in the LEP experiments, the structure of the mass matrix and relative phase among scalar quarks, that is derived from the structure of the SUSY breaking and theoretical models, is most strongly constrained by the neutron EDM upper bound.

The measurement of the neutron EDM is one of the most efficient approach to study the off-diagonal components of the mass matrix of new particles, their mixing angles and relative phases, while the LHC experiment is the direct approach to study the diagonal components. The neutron EDM measurement at the precision frontier and the LHC experiment at the high energy frontier are complementary to each other to study the new physics beyond the standard model. In some cases in the framework of the SUSY and the large extra dimension, there is a possibility in the neutron EDM measurement to probe new particles beyond the 5 TeV where even the LHC cannot reach. In addition, the value of neutron EDM larger than 10^{-28} e-cm, which is

two orders of magnitude below the present upper bound, is often predicted in the case the mass of the new particle is in the range of a few hundred GeV. However, we need to pay attention that smaller values can be also predicted choosing the mass and the relative phase. Such model dependence is common to indirect approaches such as the EDM and the LFV, which probe high energy phenomena at the loop level. We can most efficiently study the TeV-scale physics up to the GUT-scale physics by combining the determination of the mass scale of new particles at the LHC together with the EDM and LFV searches with the improved experimental sensitivity by one or two orders of magnitude.

3 Neutron EDM Measurement

The EDM is measured as the dependence of the frequency of the neutron spin precession under the magnetic field \mathbf{B} and the electric field \mathbf{E} . The precession frequency ν is given as

$$h\nu = -2\boldsymbol{\mu}_n \cdot \mathbf{B} - 2\mathbf{d}_n \cdot \mathbf{E}, \quad (2)$$

where $\boldsymbol{\mu}_n$ and \mathbf{d}_n are the magnetic and electric dipole moments of neutrons. Both $\boldsymbol{\mu}_n$ and \mathbf{d}_n are parallel or antiparallel to the neutron spin. The change in the precession frequency signals a non-zero value of the neutron EDM when the electric field is applied parallel and antiparallel to the magnetic field.

The frequency change is measured as the phase difference of the neutron polarization after the spin precession for a fixed time T .

$$\begin{aligned} \Delta\phi &= (\nu_+ - \nu_-)T, \\ h\nu_{\pm} &= 2(\mu_n B \pm d_n E). \end{aligned} \quad (3)$$

The statistical sensitivity to the neutron EDM is given as

$$\sigma_{d_n} = \frac{\hbar/2}{\alpha ET\sqrt{N}}, \quad (4)$$

where N is the number of detected neutrons and α is the quality factor of the experimental setup including the neutron polarization and the analyzing power of the neutron polarization.

The 50-year history of the search for the neutron EDM is shown in Fig. 2. The experimental sensitivity was remarkably improved after the successful storage of UCNs. The UCN is defined as the neutrons sufficiently slow to be totally reflected by the Fermi potential on the material surface and to be confined in a material bottle. The Fermi potential of the nickel amounts $U \sim 250$ neV, which is often referred to as the typical energy range of UCNs. The corresponding critical velocity is $v_c = 7$ m s⁻¹.

The improvement of the experimental sensitivity is almost saturated since recent results were delivered

by the same UCN beam at the research reactor of the Institut Laue Langevin. Their UCNs are obtained by decelerating very slow component on the tail of the Boltzmann distribution using the gravity and the mechanical doppler shifter.

New generation UCN sources are expected to increase the UCN intensity in orders of magnitude, which enables another remarkable improvement of the experimental sensitivity and may reach the discovery of new physics. Most of them are superthermal UCN sources, which decelerate neutrons via inelastic scattering in a medium. In addition, accelerator-based spallation neutron sources are beginning to accommodate the UCN source. Spallation neutron sources are compact so that a large solid angle can be covered by decelerator medium.

A superthermal spallation source, which is capable of supply 1000 UCN/cm^3 to instruments, is under commissioning at the Paul Scherrer Institute in Switzerland and is getting ready for the physics run in this year aiming to reach the sensitivity of $5 \times 10^{-27} \text{ e}\cdot\text{cm}$ by 2012. They are going to extend to the sensitivity of $6 \times 10^{-28} \text{ e}\cdot\text{cm}$ by 2015. Another superthermal spallation source for the UCN source density of 10^4 UCN/cm^3 will be constructed at TRIUMF in Canada. A superthermal converter from cold neutrons to UCNs at the Spallation Neutron Source in Oak Ridge is at the R&D phase aiming to reach $10^{-28} \text{ e}\cdot\text{cm}$. More UCN sources are under commissioning, construction at ILL, Munich FRM-II, LANL, etc. The UCN intensity is absolutely important for the excellent experimental sensitivity. However, we must overcome the barrier of the systematic errors.

In addition, atomic EDM searches are continuously improved and searches for the deuteron EDM and muon EDM are coming into the design phases. EDM measurements of various particles are complementary to each other since each of them carries the information of the fundamental CP phases in a different way. Among these,

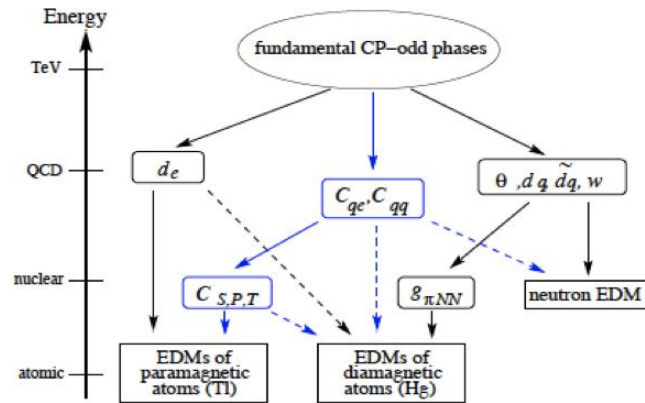


Figure 1: Relation among the EDM of various particles.

the deuteron EDM has a remarkable sensitivity to new physics via the pion exchange contribution between proton and neutron, and the experimental search at the level of $10^{-29} \text{ e}\cdot\text{cm}$ is aiming to start physics run in 2016 on the basis of the frozen spin method [2].

Returning to the neutron EDM, the best upper bound $|d_n| \leq 2.9 \times 10^{-26} \text{ e}\cdot\text{cm}$ (90% C.L.) [3] was obtained from the result of

$$d_n = (+0.2 \pm 1.5(\text{stat}) \pm 0.7(\text{syst})) \times 10^{-26} \text{ e}\cdot\text{cm}. \quad (5)$$

The result implies that the systematic error must be suppressed to go below 10^{-27} e-cm to reach into the region of 10^{-28} e-cm.

In the proposed experiment, we are going to suppress the systematic error with existing technologies, that is, the optical control to deliver dense UCNs into a smaller storage volume and reach 6×10^{-28} e-cm with minimum innovations.

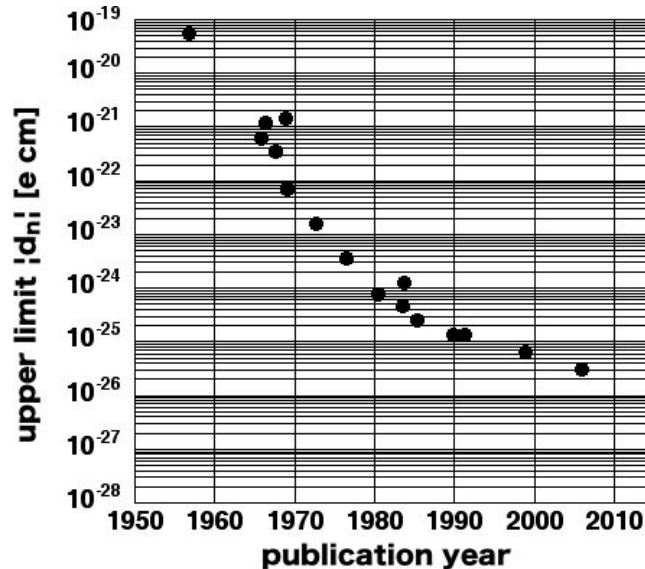


Figure 2: History of experimental upper bounds on neutron electric dipole moment.

3.1 Systematic Errors

The neutron EDM is related to the Larmor frequency ν_{\pm} , the applied electric field E , and the residual magnetic field B according to Eq. 3, and the background against the EDM signal is caused by the interaction between μ_n and B . Most part of the background can be canceled out by taking a difference between ν_+ and ν_- , and the systematic error of the measured value of d_n arises from the difference between the residual magnetic fields with the parallel and antiparallel electric fields. Using the known value of the magnetic moment of the neutron of $\mu_n = -6.029776 \times 10^{-8}$ eV/T, the difference of the residual magnetic fields for the parallel and antiparallel electric fields should be reduced to be less than 140 aT in order for the magnetic background to be smaller than the EDM signal with an expected sensitivity of $d_n = 0.7 \times 10^{-27}$ e-cm and the applied electric field strength of $E = 12$ kV/cm. Our co-magnetometer technique has already achieved the sensitivity of about 100 aT, which is enough for checking the above mentioned magnitude of the residual magnetic field.

The residual magnetic field consists of the background magnetic field B_{BG} and the induced magnetic field B_S due to the motion of the neutron in the applied electric field E , and it is crucial to suppress both B_{BG} and B_S for the high precision measurement of d_n . As the possible sources of B_{BG} , one should consider the following

effects:

- a) penetration of the magnetic field from a permanent magnet located at the neutron entrance door,
- b) penetration of the magnetic fields due to the other components around the UCN cell,
- c) quadrupole field caused by the gradient of the residual magnetic field,
- d) uncompensated drift of the magnetic field in the measurement with the ^{199}Hg co-magnetometer, and
- e) induced magnetic field by a leakage current between high-voltage electrodes.

The above effects have been studied in the experiments at ILL [3] and PSI [4, 5], and have been evaluated as summarized in Table 1. In this evaluation, we assumed that the storage volume is 1000 cm^3 . Since the uncertainties of those effects are essentially due to their position dependencies or spatial nonuniformities which cannot be removed in the difference between ν_+ and ν_- , they can be approximated with linear functions of the spatial dimension in the lowest order, and are to be suppressed by using a smaller UCN storage cell. Assuming the uncertainties to be proportional to the linear dimension of the UCN storage cell, and comparing the size of the present cell (1000 cm^3) with the one employed in the PSI experiment (21000 cm^3), the errors concerning B_{BG} are expected to be reduced as shown in Table 1.

For B_S , we took into account the following components:

- f) the magnetic field B_{ST} induced by the net translational motion of the neutrons,
- g) the magnetic field B_{SR} induced by the net rotational flow of the neutrons, and
- h) the magnetic field B_{SS} due to second-order corrections for B_{ST} and B_{SR} .

Here B_{ST} is proportional to the vector product of the net translational velocity v_T and the applied electric field E , where v_T is caused by the ascent of the center-of-mass of the neutron gas due to the heating during the Ramsey measurement period. Since the heating of the neutron gas is governed by the collisions with the ^{199}Hg atoms for the co-magnetometer or the inner wall of the UCN storage cell, the effect is expected to be proportional to the density of the ^{199}Hg gas as well as the collision rate per target atom. In the proposed experiment, the gas density will be adjusted to be $3.0 \times 10^{10}\text{ atoms/cm}^3$, which is the same as the previous experiments. On the other hand, although the mean neutron velocity in the proposed experiment is smaller than that in the previous experiments, the collision rate will be unchanged because the scattering cross section can be assumed to be proportional to the inverse of the neutron velocity. Consequently, B_{ST} is expected to be comparable with the value in the previous experiments. For B_{SR} and B_{SS} , their effects may be reduced because of the smaller neutron velocity, but here we assumed them to be the same as the PSI experiment for a conservative evaluation.

	Effect	Shift	σ at ILL	σ at PSI	σ at J-PARC (storage volume 1000 cm ³)
a	Door cavity dipole	-5.6	2.0	0.10	0.036
b	Other dipole fields	0.0	6.0	0.40	0.14
c	Quadrupole difference	-1.3	2.0	0.60	0.22
d	Uncompensated B drift	0.0	2.4	0.90	0.33
e	Leakage currents	0.0	0.1	0.10	0.036
f	$v \times E$ (translational)	0.0	0.03	0.03	0.030
g	$v \times E$ (rotational)	0.0	1.00	0.10	0.10
h	Second-order $v \times E$	0.0	0.02	0.02	0.02
i	ν_{Hg} light shift (geo phase)	3.5	0.8	0.40	0.17
j	ν_{Hg} light shift (direct)	0.0	0.2	0.20	0.20
k	Hg atom EDM	-0.4	0.3	0.06	0.06
l	Electric forces	0.0	0.4	0.40	0.14
m	ac fields	0.0	0.01	0.01	0.01
Total		-3.8	7.2	1.31	0.53

Table 1: Summary of systematic errors (10^{-27} e-cm).

In addition to the above considered effects of the residual magnetic field, the systematic errors will arise from the following sources:

- i) the light shift of the Larmor frequency of the ^{199}Hg atom via a geometric phase,
- j) the direct light shift of the Larmor frequency of the ^{199}Hg atom,
- k) the uncertainty of the absolute value of the ^{199}Hg atomic EDM,
- l) electric forces between the high-voltage electrodes, and
- m) residual ac fields.

In the above sources of the systematic errors, the light shifts of the Larmor frequency of ^{199}Hg depend on the atomic EDM of ^{199}Hg , and therefore their uncertainties are improved by employing the most recent data of the ^{199}Hg atomic EDM [6].

The electric forces may move the high-voltage electrodes in the gradient of the magnetic field, and may generate an EDM-like signal. It is supposed to be approximately proportional to the change of the spacing between the electrodes, and in the proposed experiment, its effect will be the same as in the ILL experiment because of the similar setup of the electrodes.

Finally, the ac field due to the noise of the applied high voltage may also generate an EDM-like signal. From the experience in the previous experiments, the noise level should be reduced down to 50 V for the high voltage of 12 kV in order to suppress its contribution to be less than 10^{-29} e-cm.

3.2 Statistical Error

The downsizing of the storage volume increases the collision frequency of UCN on the storage wall and decreases the storage time τ . The statistical sensitivity (σ_{d_n} in Eq. 4) is minimized when $T = 2\tau$. Thus the measurement time T is decreased if the storage time τ is decreased. The disadvantage can be minimized by adjusting the storage volume L^3 and the maximum UCN velocity v_{\max} .

- The beam time available at the J-PARC is 5000 hours per year. The achievable statistical error in one year is $(\Delta d_n)_{\text{stat}}^{\text{year}} = \sigma_{d_n} \times (5000\text{hours}/T)^{-1/2}$.
- The T is proportional to the L and inversely proportional to the v and loss probability on the wall. It can be shown that the loss probability on the wall is proportional to $v^{3-\gamma}$. Here we put the dependence of the loss probability on the wall surface on the UCN velocity v is proportional to $v^{-\gamma}$, where $\gamma \sim 1$ when UCN receives thermal energy from surface atoms, and $\gamma \sim 0$ when UCN scarcely does.
- The N is proportional to $L^3\rho$ where ρ is the UCN density. The UCN density is proportional to v_{\max}^3 assuming the phase space density is uniform in the UCN region.

Consequently, we obtain

$$(\Delta d_n)_{\text{stat}}^{\text{year}} \propto L^{-2} v_{\max}^{-(\gamma+3)/2} \rho_0^{-1/2}, \quad (6)$$

where ρ_0 is the density of UCN of $0 < v_{\max} \leq 7$ m/s.

We expect the $\rho_0 \sim 3100 \text{ cm}^{-3}$ (see § 3.3.1) by introducing the neutron rebuncher described in § 3.3.2. The estimation of the systematic and statistical errors are shown as a function of L for several values of v_{\max} in Fig. 3 together with the systematic error as a function of L assuming the same co-magnetometer sensitivity as previous experiments. The accuracy at the level of 10^{-27} e-cm will be achieved in one year.

The systematic and statistical errors with 30 times larger UCN density ($\rho_0 \sim 93000 \text{ cm}^{-3}$) are also estimated as shown in Fig. 4. The very large UCN density can be obtained by developing the neutron condenser combining the neutron rebuncher and the neutron juggler described in § 3.5. In this case, we can reach the accuracy of 6×10^{-28} e-cm in one year.

3.3 UCN Source

We propose to employ a dedicated pulsed spallation neutron source to concentrate the UCN production in time and to transport the pulsed UCNs into the EDM measurement volume using the neutron magnetic optics (cf. Fig. 5). The J-PARC proton accelerators are the most appropriate driver for this purpose. In the proposed experiment, we assume the 400 MeV proton beam with the peak current of 50 mA and the pulse width of 0.5 ms with the repetition rate of 0.5 Hz, which can be branched from the J-PARC LINAC in the same manner as already discussed in Ref. [1].

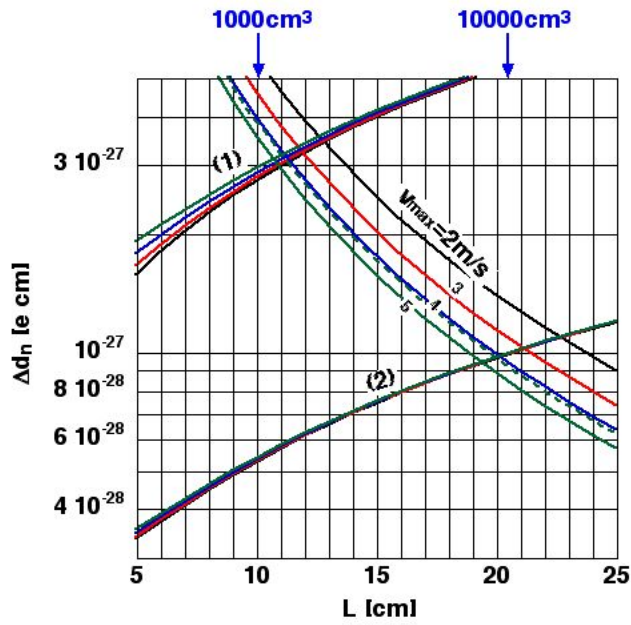


Figure 3: Estimated experimental accuracy is shown as a function of the size of the EDM measurement bottle filled with the density of 3100 cm^{-3} at the beginning of the precession. The lines labeled as (1) and (2) are the systematic errors extrapolated from the error sources of existing experiments at ILL and PSI. Solid lines from left-top to right-down are statistical errors for $\gamma = 1$ and dotted lines for $\gamma = 0$. Black, red, blue and green lines corresponds to $v_{\text{max}} = 2, 3, 4, 5 \text{ m/s}$, respectively.

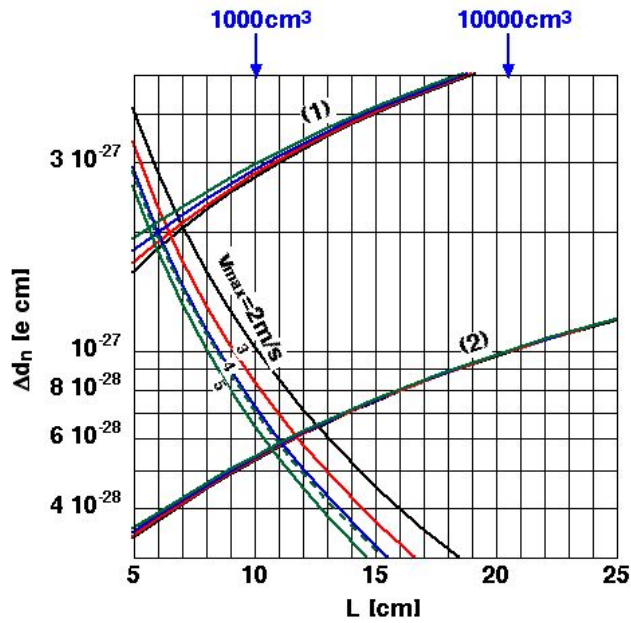


Figure 4: Estimated experimental accuracy when the UCN density is 30 times increased ($\rho = 93000 \text{ cm}^{-3}$).

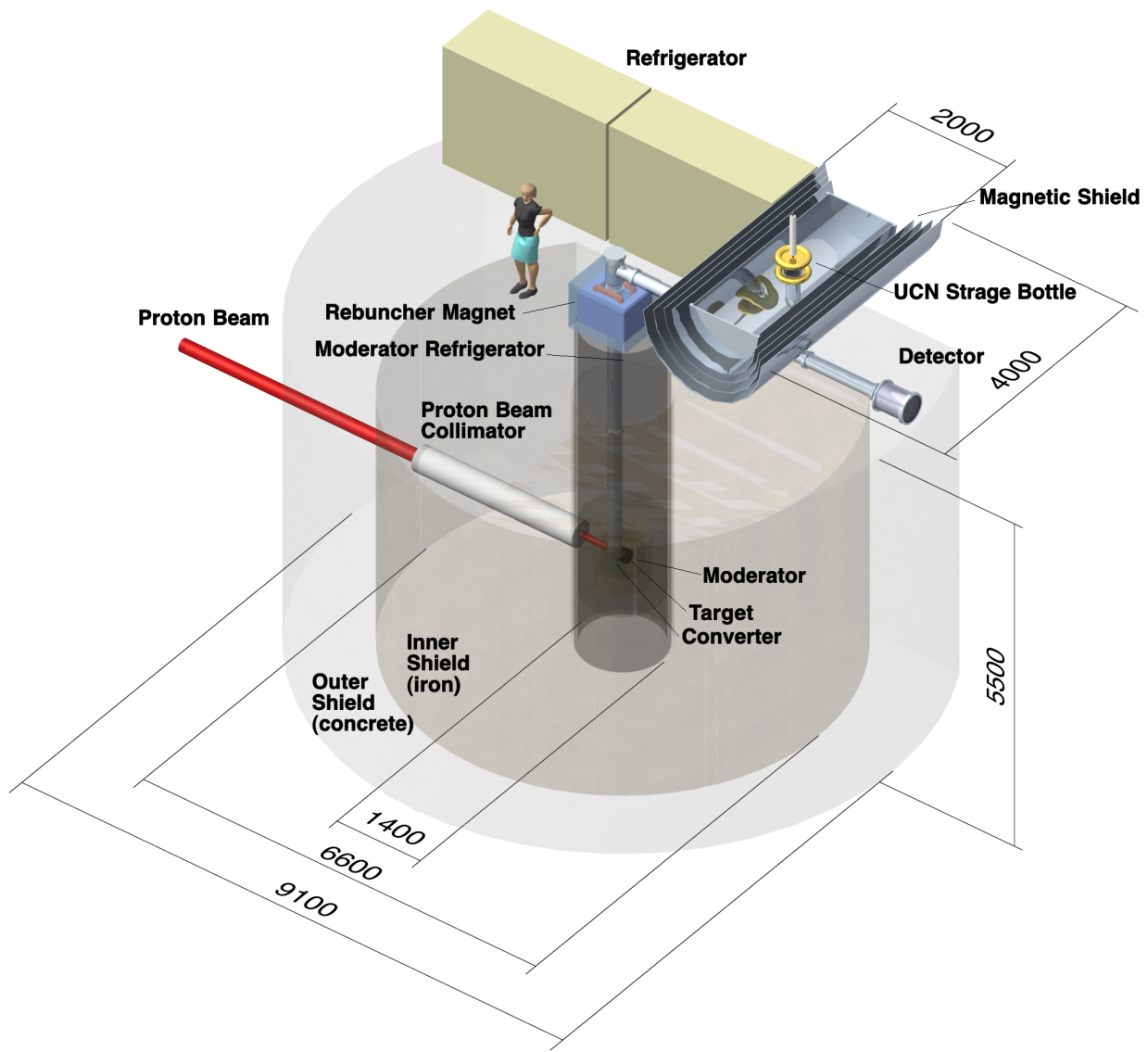


Figure 5: The ultracold neutron source at the J-PARC for the measurement of the neutron electric dipole moment.

3.3.1 UCN Converter

The disadvantage of the downsizing of the storage volume and the lowering the maximum UCN velocity can be compensated by increasing the UCN density in the storage volume.

UCN can be produced by cooling neutrons produced in a nuclear reaction in a spallation source. The UCN density obtained by a conventional method, in which one can extract UCNs from the tail of the Maxwell-Boltzmann distribution of the cold neutrons, is limited by Liouville's theorem. In order to overcome the problem, we will employ new method called "superthermal method" which is firstly proposed by R. Golub and J. M. Pendlebury in 1975 [7]. In the superthermal method, neutrons interact with a medium (called "converter" hereafter) that converts the cold neutrons into UCN via inelastic scattering with phonon. A medium with a large down scattering cross-section and small absorption cross-section is preferable as a converter. Several nuclei meet the above condition, but only solid deuterium (sD₂) [8] and superfluid helium (He-II) [9] converter have been demonstrated as of this proposal written. We choose the sD₂ converter for our superthermal UCN source for the smooth startup of physics experiments because its UCN production rate is the largest, well conserves the timing structure of produced UCN and well matches to the characteristics of transport optics and also is relatively easy to handle. In the following, some specific properties of the sD₂ are described.

The sD₂ has been used as the UCN converter soon after the proposal of the superthermal method because of its very small neutron absorption cross-section (520 μ barn for neutron velocity of 2200 m/s) and large scattering cross-section. A deuterium (D₂) has two molecular state, i.e. ortho and para, according to the symmetry of the wave functions for nuclear spins. At low temperature limit, all of the ortho-D₂ is in the ground state, and in contrast all of the para-D₂ is in the first excited state. The up-scattering cross section of UCN for the D₂ in the excited state is known to be 10 times larger than that for the ground state, thereby causing a large UCN loss [10, 11]. Ortho rich D₂ is therefore highly desired for the UCN converter, and up to 98% ortho-D₂ can be produced by already well established technique [12]. Although strong irradiation to the converter induces the ortho- to para-D₂ conversion, the effect would be very small in the case of the proton beam power we are now assuming. The UCN lifetime in a medium is usually not dependent on the neutron velocity because of the $1/v$ law. If an ideally pure ortho-D₂ is used for the UCN converter, the up-scattering cross section is negligibly small at 4K. The UCN lifetime is thus determined only by the neutron absorption by the D₂, that is calculated to be 140 msec.

In order to efficiently extract the generated UCN, the converter is required to be "transparent", which means that the scattering and absorption in the converter is very small. The degree of transparency is predominantly determined by the elastic scattering because the inelastic scattering is sufficiently small at below 4 K as already mentioned the above. The absorption length is 70 cm for UCN whose velocity is 5 m/s. The total cross-section of UCN for the sD₂ was measured to be 10 – 20 barn [13]. However, the total cross-section strongly depends on the crystal state; the total cross-section was increased to 50 barns after the thermal cycle test (5 K to 18 K), which is probably due to the change of the lattice. Highly transparent sD₂ crystal can be created by growing

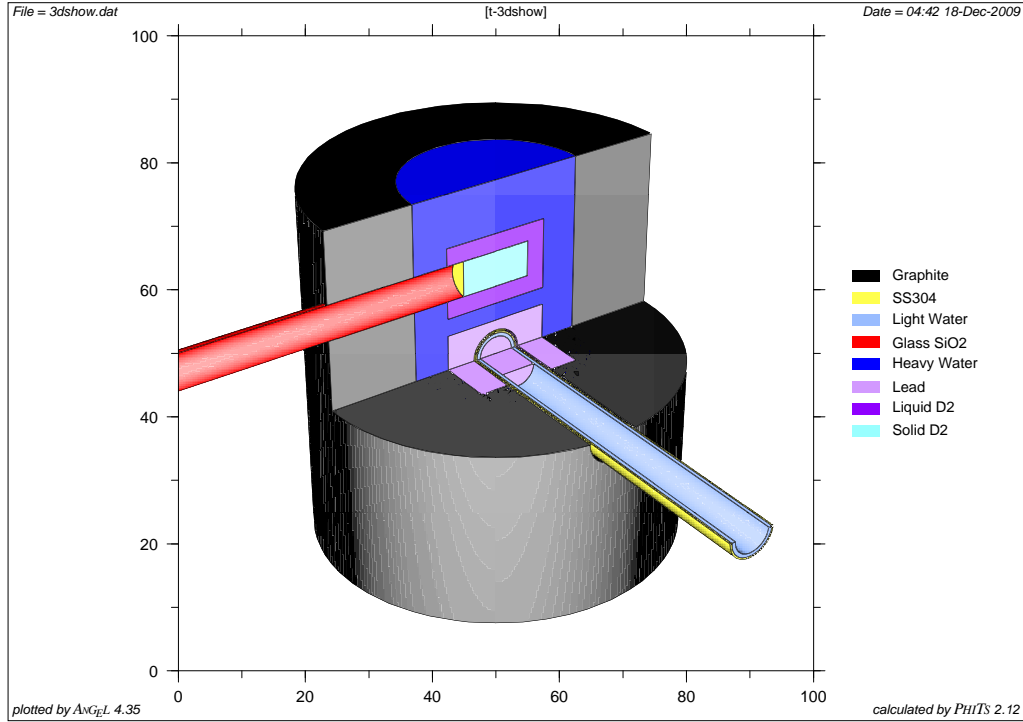


Figure 6: A schematic view of the superthermal UCN source implemented in the PHITS. See text for more detail.

directly from the gas state. Thanks to the J-PARC accelerator operated in the pulse mode, we might be possible to apply the method because of the temperature variation in the sD₂ is small.

We calculated the UCN production rate in the sD₂ converter by using a Monte Carlo simulation code, PHITS (Particle and Heavy Ion Transportation code System) [14], which is widely used in the accelerator field, the aerospace field, and so on. A schematic view of the superthermal UCN source implemented in the PHITS is shown in Fig. 6. A cylindrical sD₂ converter whose radius and height is 5 cm and 20 cm, respectively, is vertically placed above a lead neutron production target. The target is covered with a lead γ ray shield. Cylindrical 20-K liquid deuterium and 300-K heavy water surround the sD₂ converter as a neutron moderator. The 300-K heavy water is surrounded by a graphite neutron reflector. In the simulation, the incident proton beam energy, current and width are set to be 400 MeV, 50 mA and 0.5 msec, respectively.

The UCN production rate P is calculated to be $P = 1.0 \times 10^{-8} \Phi_0$ UCN/cm³/pulse [15], where Φ_0 is a flux of cold neutrons. Fig. 7 shows the energy spectrum at the sD₂ converter calculated by PHITS. According to Fig. 8 from Ref. [15], the phonon state density above 10 meV is almost zero. In order to obtain the Φ_0 , we therefore integrated the energy spectrum up to 10 meV, and the UCN production rate is then obtained to be $P = 6200$ UCN/cm³/pulse.

3.3.2 UCN Transport - Neutron Rebuncher

The density of UCN is largest in the UCN converter and it rapidly decreases after they move in the free space. Even if UCNs are traveling in parallel or traveling inside a neutron guide, the velocity difference results in

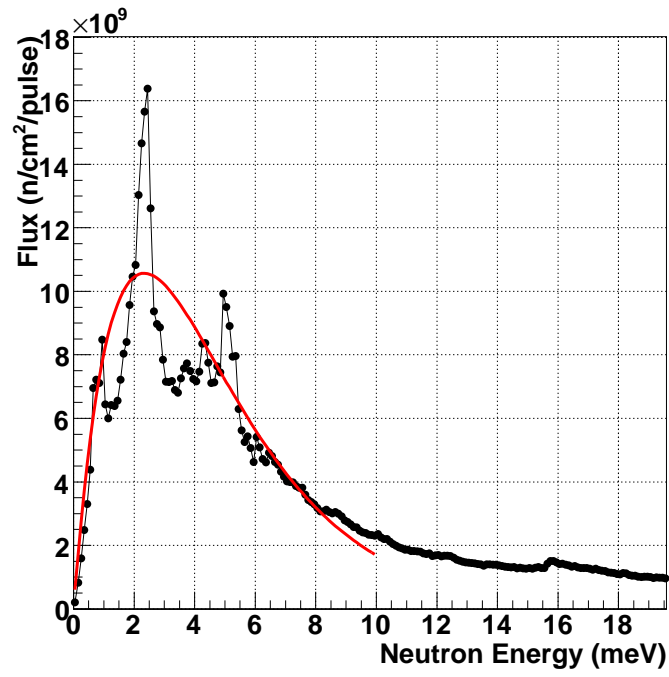


Figure 7: Energy spectrum of cold neutron at the sD₂ converter calculated by PHITS.

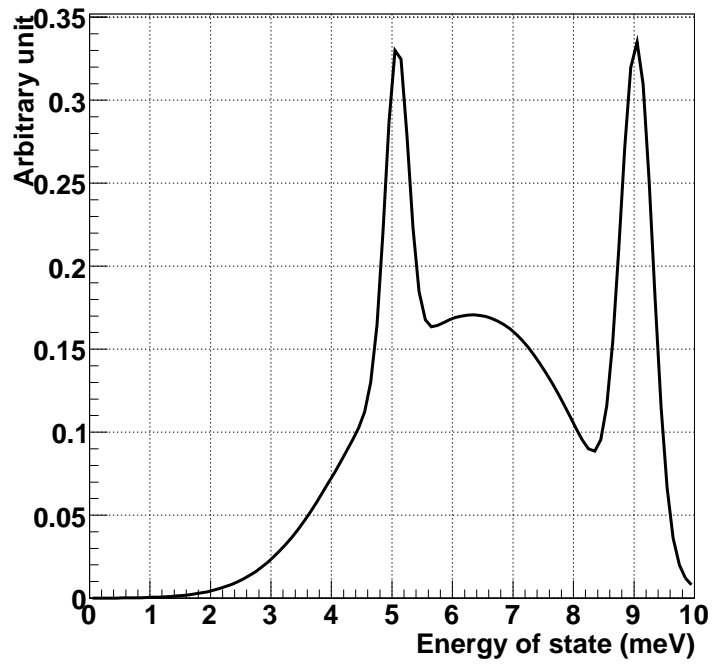


Figure 8: The phonon state density for sD₂ evaluated in Ref. [15].

the decrease of density. Therefore, we usually receive dilute UCN beam at remote experimental instrument. However, the density of pulsed neutron beam can be reproduced at a remote place by decelerating the faster neutrons and accelerating the slower neutrons. This method is referred to as the time-focusing or the rebunching. Hereafter neutron optical device to rebunch neutrons at a remote place as the "neutron rebuncher" (NR).

In the proposed experiment, a resonance spin flipper (RSF) is planned to be used as a component of the NR. A RSF generates a static magnetic field B_z and a temporarily oscillating magnetic field $B_r \cos(\omega t)$. The spin is flipped when the condition of $\hbar\omega = 2\mu B_z$ is satisfied. Neutrons are decelerated by the emission of the energy $\hbar\omega$ to the oscillating magnetic field through the spin-flip process.

We place an NR 5 m above the converter and reflect the neutrons through the NR to the horizontal direction. The shutter to the cell is at 3 m downstream from the reflector. Without using the NR, the neutron whose velocity is 10.10 m/s at the converter arrives at the equipment and the shutter 0.83 sec and 2.33 sec after the conversion, respectively.

We discuss the requirements for the NR to decelerate the neutrons with other velocities at the converter to arrive at the shutter 2.33 sec after the conversion. The neutron whose velocity is 10.62 m/s at the converter is decelerated by the gravitational field to 3.84 m/s and reaches to the NR 0.69 sec after the conversion. The NR decelerates the neutron velocity to 1.84 m/s by generating B_z of 0.49 T and corresponding oscillating field. The decelerated neutron arrives at the shutter 2.33 sec after the conversion. Therefore, to decelerate neutrons depending on their velocity. B_z have to be reduced from 0.5 T to 0 T in $0.83 - 0.69 = 0.14$ sec. Fig. 9 shows the rebunching process in space-time coordinate. Red and blue lines represent the flight path of fast and slow neutrons, respectively.

The bunch size near the shutter is equal to that near the converter. Therefore, the bunch size is 3 cm when the thickness of the converter is 3 cm. In this case, we have to open the shutter for 0.16 sec so that the whole bunch with the velocity of 1.84 m/s passes the shutter. If we assume the bunches are generated every 0.50 sec, $0.16/0.50 = 0.34$ part of the neutrons in the cell escape while adding one neutron bunch. Repeating the procedure for 10 times, the number of neutrons in the cell becomes 2.9 times larger than that is obtained when we do not use the NR and open the shutter only once. This density gain saturates as shown in Fig. 10.

The UCNs are accumulated on the bottom of the EDM measurement instrument. These UCNs are lift up into the EDM measurement bottle by the neutron elevator.

3.3.3 Proton Beam Availability

The J-PARC linear accelerator (LINAC) is capable of providing pulsed proton beams with the repetition rate of 50Hz, while it is currently providing protons to the 3 GeV Rapid Cycle Synchrotron (RCS) with the repetition rate 25Hz. For the superthermal UCN source, proton beams with the repetition rate of 0.5Hz is necessary (see § 3.3.2). Such proton beam is available by branching the LINAC beam under normal operation. In this case the beam delivery to the RCS is lost by 2%. Another method, which is by filling up the vacant packet under

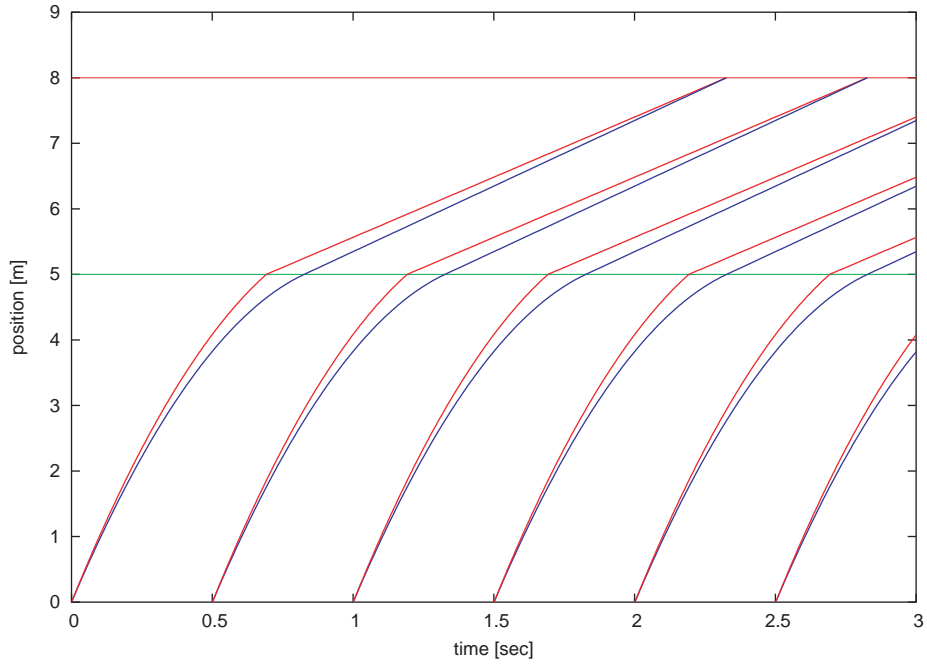


Figure 9: Rebunching process in the space-time coordinates.

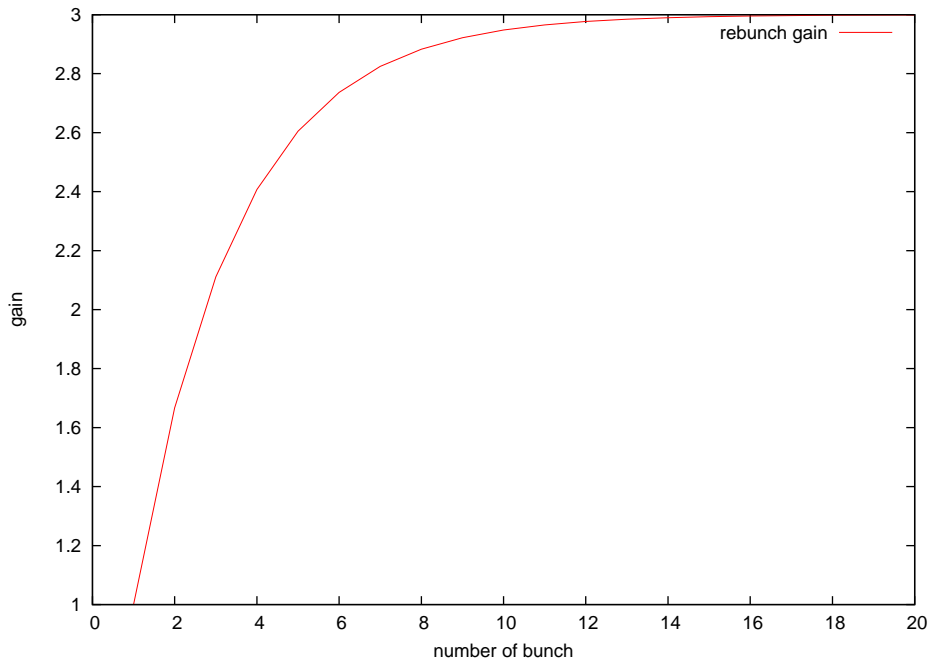


Figure 10: Gain saturation curve.

50Hz to branch additional protons up to 250kW, has been discussed in order not to disturb the beam delivery to the RCS [1].

3.4 Magnetometry

In order to detect/measure an EDM of neutron with sensitivities intended in the present proposal, the magnetometry is of exclusive importance. This is because the measurement of an EDM is nothing other than the determination of a tiny change in the precession frequency of spin due to the application of an electric field, and the spin precession is far more sensitive to a magnetic field. A $\delta d \sim 10^{-27}$ e-cm sensitivity, for example, for an EDM measurement with a ± 10 kV/cm electric field requires control of the magnetic field acting on the spin to $\delta B \sim 300$ aT. In the present proposal we will adopt and install in the EDM cell a magnetometer based on the nonlinear magneto-optical rotation (NMOR) effect, which should achieve sensitivities of the order of 100 aT or better. In fact, a high-sensitivity NMOR magnetometer is under development for use in a planned experiment for the ^{129}Xe atomic EDM by T. I. Tech-RIKEN group, and therefore the magnetometer development for the present proposal may be pursued in an intimate cooperation with them.

3.4.1 NMOR magnetometer

We plan to employ a magnetometer based on the nonlinear magneto-optical rotation (NMOR) effect [16]. It provides sensitivities that are by one order of magnitude higher than those achieved with optical pumping magnetometers discussed in § 3.4.2 below.

The principle and setup for the NMOR magnetometer are as follows: A linearly polarized light, of wavelength of the Rb D1 line, passes through a volume which is filled with a thin vapor of Rb ($\sim 10^9$ atoms/cm³). Being irradiated by the linear polarized light the Rb spins are aligned in a direction perpendicular to the axis of light propagation (the z-axis), as illustrated in Fig. 11. If there is a magnetic field B acting on the atoms in the z-direction, the spin alignment rotates about the z-axis because of the precession of the Rb spins. The rotation of spin alignment, in turn, induces rotation of the plane of linear polarization for the transmitted light. Thus, a light (which has been linearly polarized in the x-direction when entering the Rb vapor) transmitted through a Rb vapor acquires rotation of its plane of polarization by an angle ϕ , as shown in Fig. 12. The magneto-optical rotation ϕ is a nonlinear function of B , with its slope around $B \sim 0$ being remarkably steep when the spin coherence time is long. Coherence times τ_{coh} as long as ~ 6 ms and width ΔB [the magnetic field difference between the peak and valley of the dispersion-like curve for $\phi(B)$] as narrow as ~ 300 nT have been obtained already by the T. I. Tech-RIKEN group, by performing a Paraffin coating of the inner surface of a glass Rb cell. The world-best result is $\tau_{coh} \sim 1$ s [17] enabling a sensitivity of 300 aT/Hz^{1/2}. We thus set a goal presently at 300 aT/Hz^{1/2}, or a field measurement with sensitivities $\delta B \sim 100$ aT with narrowed bandwidths of $0.1 \sim 0.01$ Hz.

A schematic setup for a planned NMOR magnetometer is illustrated in Fig. 13.

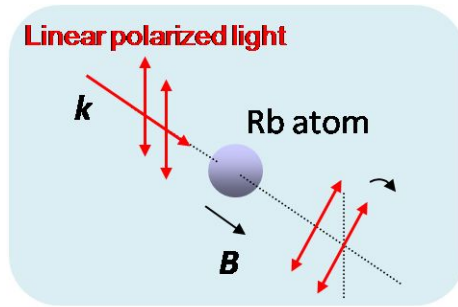


Figure 11: Rotation of the plane of polarization due to precession of Rb spins under an external magnetic field B .

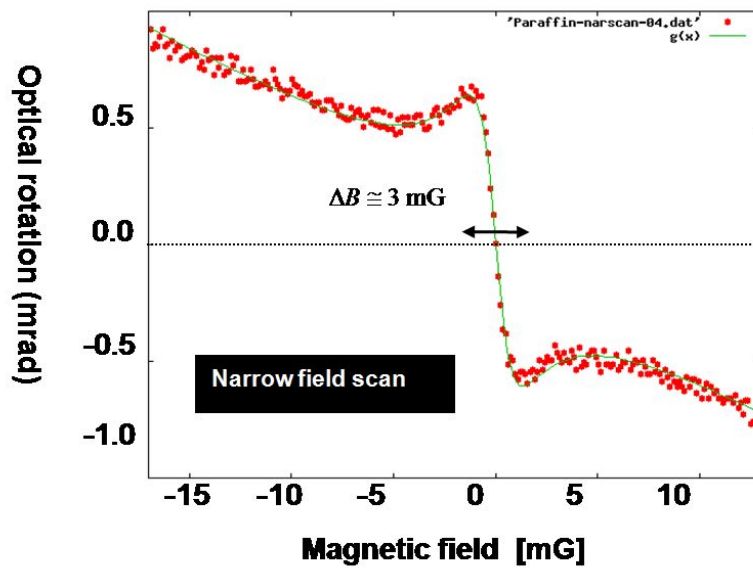


Figure 12: Optical rotation angle ϕ as a function of the magnetic field B .

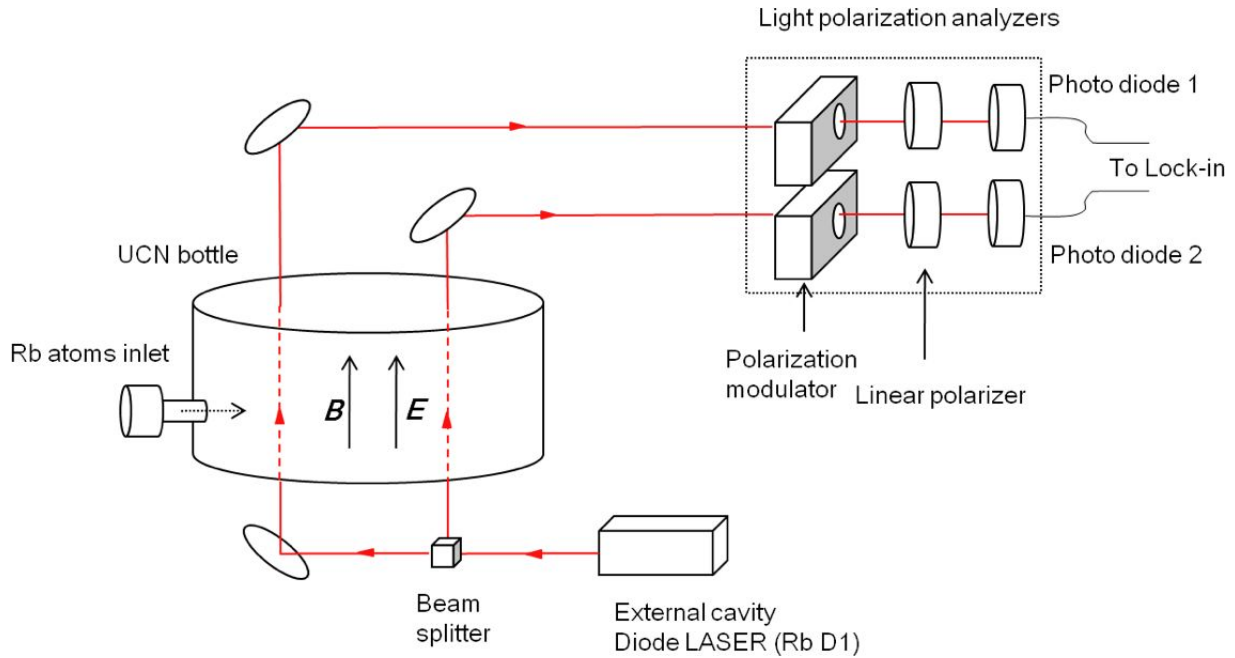


Figure 13: Schematic illustration of the experimental setup of a planned NMOR magnetometer.

3.4.2 Magnetometers in other EDM experiments

Up to now a few types of magnetometer have been or are planned to be employed in neutron EDM experiments:

- (a) Hg magnetometer
- (b) Cs magnetometer
- (c) ^3He magnetometer
- (d) SQUID magnetometer

The first three are all so-called optical pumping (OP) magnetometers which involves polarization of spins via optical pumping and succeeding spin detection for the determination of the precession angle. Their achieved or expected sensitivities are of order of (a) 100 fT, (b) 3 fT, (c) 1 fT. The SQUID magnetometer (d) is expected to achieve a sensitivity $\sim 80 \text{ aT/Hz}^{\frac{1}{2}}$ when combined with a high-Q resonator, but requires cryogenics at the liquid He temperature and also is delicately sensitive to vibrations, thus inevitably introducing substantial complications to the experimental setups.

3.4.3 Problems to be solved or clarified

(a) It is absolutely preferable to perform magnetometry with a sensing volume that coincides with the volume where neutrons are stored (co-magnetometer). Then, a few questions arise:

- Is it possible to do the NMOR measurement in a neutron storage cell?

We have to look for a treatment of the inner surface of the storage cell that allows both a long spin coherence time for Rb atoms and a long storage time for ultracold neutrons at the same time.

- Does co-existing neutrons interfere with the Rb spins?

Since anticipated density of neutron of $\sim 10^4$ UCNs/cm³ is orders of magnitude lower compared with density of Rb of $\sim 10^9$ /cm³, the presence of neutrons may not interfere with Rb. This problem, however, needs to be worked out more carefully.

(b) We note finally that in EDM experiments the applied magnetic field B is finite (typically on the order of $1\mu\text{T}$), and what the magnetometer should perform is to measure a finite field (but not the zero field) with 100 nT sensitivity. This can be achieved by operating the NMOR with a laser light which is modulated in intensity or in wavelength [17].

3.5 Further Increase of the UCN Density - Neutron Juggler and Neutron Condenser

A direct method to increase the UCN density is to confine them inside the UCN converter. However, the absorption by the converter does not allow a large enhancement in most cases. There is another solution in the case of periodic pulse source, which is to let UCNs travel in non-absorptive region for a while and let them come back to the converter region at the next production timing. In this case, the UCNs produced in the first pulse and those in the second pulse occupies the same phase space, which results in the increase of phase space density. We refer to the device to let UCNs travel out of the moderator and come back after a certain amount of time as the "neutron juggler". If the timing of the traveled UCNs is common to all UCNs, the density enhancement is maximized. This situation can be realized by employing the neutron rebuncher. Therefore, the pulsed UCN can be condensed by combining the neutron rebuncher and neutron juggler, which is referred to as the "neutron condenser". We explain the neutron condenser in the practical case below.

For superthermal source, the maximum UCN density ρ is described as $\rho = P \times \tau$ where P is the production rate, and τ is UCN lifetime in the converter. In case of D₂ converter, the limit of τ in is 140 ms when all loss is nuclear absorption. Thus the width of incident proton beam should be longer than 140 ms to achieve the maximum density. However, the beam width is limited to 0.5 ms by the constraint from accelerator. Hence, ordinal storage only can achieve averaged beam power, which is $0.5 \text{ ms}/140 \text{ ms} = 1/280$ of the limit from statistical mechanics. Here, we propose a new idea to use the peak intensity of pulse neutron source.

First, the UCNs launched up are focused on certain position by rebuncher. Then the focused UCNs are reflected by a mirror without passing and return to the converter. It is possible to send all UCNs at a same position at same time without wavelength dependency by operating rebuncher oppositely for UCNs returning. If the UCN arrival is controlled to on converter at the same moment with the next pulse, the phase space of UCNs returning overlap with UCNs produced by next pulse. Then the UCN density becomes double in the

converter. By repeating this procedure, named "UCN Juggling", UCN density is going to be equilibrium where UCNs returning and UCN produced are same number. UCN density on the top of juggler, after n times juggling, ρ , can be described as follows;

$$\begin{aligned}\rho &= \rho_0 + \rho_0 r^1 + \rho_0 r^2 + \cdots + \rho_0 r^n \\ &= \rho_0 \left(\frac{1 - r^{n+1}}{1 - r} \right)\end{aligned}$$

Where ρ_0 is UCN density in converter with single proton pulse, r is probability to survive by a juggling. Thus, figure of merit of juggling is $1/(1 - r)$ with $n \gg 1/(1 - r)$. Note that only one spin state (parallel or anti-parallel) can storage using the magnetic rebuncher. The survival probability, r , is described as $r = (\text{mirror efficiency}) \times (\text{rebuncher efficiency}) \times (1 - \text{loss in converter})$. The mirror efficiency can be more than 99% for UCN. The rebuncher efficiency might be constrained by the flipper efficiency or depolarization, however it is known that they can be achieved over 99% for cold neutron [18]. Nuclear absorption of neutron is inevitable loss for juggling. For D_2 converter, it is 140 ms, which corresponds to attenuation length of 70 cm for UCN with 5 m/s. Additionally, if we only store one spin state by the way of like magnetic rebuncher, the spin exchanging scattering can be the significant loss. The elastic scattering only change the direction of UCN so it does not cause the loss if UCN energy is less than critical potential of the guide wall. Loss by inelastic scattering is suppressed if the converter is cold enough. However, the spin exchange reaction by incoherent scattering loses UCN from the storage. Assuming the spin exchange incoherent scattering cross section is 1.0 barn, the attenuation length in the converter is 16 cm. If we use converter of 1 cm thickness, $r = 1 - 1/8 = 7/8$, so the gain by juggling achieves to 7.4 for 20 times of juggling. With 2 Hz operation, the filling time of juggling is 10 sec. For present setup, the gain of juggling is limited by spin incoherent scattering. If we use spin independent rebuncher, or else, use converter whose nuclear spin is 0 (e.g. ^4He , $^{16}\text{O}_2$, or ^{208}Pb), spin exchange reaction can be suppressed. In that case, UCN density is growing up to the statistical UCN density, $P \times \tau$.

4 Schedule

The design and simulation will be carried out in 2010 and 2011. UCN related components will be developed and tested in 2010 and 2011. We expect to reform and construct the building to accommodate the proton beam transport and neutron production target in 2011-2012, which requires approximately 18 months (without contingency) to get ready to receive proton beam in 2013 as soon as the end of the commissioning of the energy recovery of the J-PARC LINAC. The UCN source will be under commissioning using the solid deuterium converter with the neutron rebuncher in 2013. The data production run will be started as soon as the commissioning will finish in the end of 2013. The experimental sensitivity reaches $\Delta d_n \sim 10^{-27}$ e-cm with 5000 hour operation time, expected to be in the end of 2014 or 2015.

The neutron juggler and appropriate UCN converter (null-spin material) will be studied in the period of

2010 to 2014. We start the commissioning of neutron condenser by combining the null-spin UCN converter, neutron juggler and neutron rebuncher as soon as the physics run reaches to $\Delta d_n \sim 10^{-27}$ e-cm. We assume a half-year commissioning for the operation of the neutron condenser. We restart the physics run in 2015-2016 to reach 6×10^{-28} e-cm using approximately 5000 hour beam time.

1. UCN Test Port at the J-PARC MLF

A doppler shifter currently under development will be ready in the 2nd quarter of 2010 under the collaboration among Kyoto University, University of Tokyo and KEK. Large critical angle supermirrors to reflect very cold neutrons from the J-PARC MLF BL05 beam port are under design process and will be fabricated at the Research Reactor Institute of Kyoto University in the 1st quarter of 2010. The doppler shifter will be assembled in the 2nd quarter and tested in 2010. In the earliest case, UCN beam will be ready for testing UCN detectors, UCN reflectivity study and prototyping the neutron rebuncher in the 2nd quarter of 2010.

2. Neutron Rebuncher

The prototype will be constructed in 2010 and 2011 in Kyoto University and tested at the UCN test port at the J-PARC MLF BL05 under the collaboration between Kyoto University, Japan Atomic Energy Agency and KEK. The UCN spin flipper will be tested in this process. They are the world-leading specialists in neutron spin optics, which are applied in neutron spin interferometer based on multilayer mirror assembly, neutron spin echo for soft-matter research and magnetism researches.

3. UCN Storage Bottle

Appropriate wall material will be studied in 2010 and 2011 in Osaka University and Kyoto University. The bottle should have a long storage time, magnetism free, voltage proof.

4. Magnetometer

The improvement of the magnetometer will be done in 2010 through 2012 under the initiative of Tokyo Institute of Technology.

- Achieving sensitivities of $\delta B \sim 100$ fT in a prototype setup \rightarrow In 0.5 year after the start of this project.
- Achieving sensitivities of $\delta B \sim 100$ aT in a prototype setup \rightarrow In 1.5 year after the start of this project.
- Realizing a modulated NMOR magnetometry for finite fields \rightarrow In 2 year after the start of this project.
- Installing to the neutron storage cell \rightarrow In 3 year after the start of this project.

5. Proton Beam Transport

We would ask KEK and JAEA to manage the proton beam delivery to the UCN source, necessary con-

structions including constructing additional building or tunnel to accommodate the system. In addition, we also ask KEK and JAEA to provide the radiation shield and the safety systemization of the target system together with the operation staffs.

6. UCN Source

The UCN source will be designed and constructed under the collaboration among KEK Laboratories (Institute of Particle and Nuclear Studies, Accelerator Lab., Neutron Science Lab., Radiation Science Center, Cryogenics Science Center), Hokkaido University, Japan Atomic Energy Agency.

7. UCN Transport

The UCN guide and lifter will be developed under the collaboration between Kyoto University and KEK.

8. Neutron Juggler and Null-spin UCN Converter

Fundamental studies will be carried out by Hokkaido University, Kyoto University, University of Tokyo and KEK.

5 Research Group

Hirohiko M. SHIMIZU	KEK
Takashi INO	KEK
Suguru MUTO	KEK
Tamaki YOSHIOKA	KEK
Kenji MISHIMA	KEK
Yasushi ARIMOTO	KEK
Kaoru TAKETANI	KEK
Hiroshi IWASE	KEK
Toru OGITSU	KEK
Nobuhiro KIMURA	KEK

Sachio KOMAMIYA	Dept. Phys., Univ. Tokyo
Satoru YAMASHITA	ICEPP, Univ. Tokyo
Yoshio KAMIYA	ICEPP, Univ. Tokyo

Yoshihisa IWASHITA	Inst. Chem. Res., Kyoto Univ.
Masahiro HINO	Research Reactor Institute, Kyoto Univ.
Masaaki KITAGUCHI	Research Reactor Institute, Kyoto Univ.
Hiroyuki FUJIOKA	Dept. Phys., Kyoto Univ.

Tatsushi SHIMA	Research Center for Nuclear Physics, Osaka Univ.
Masahiko UTSURO	Research Center for Nuclear Physics, Osaka Univ.

Kenji SAKAI	Japan Atomic Energy Agency
-------------	----------------------------

Koichiro ASAHI	Tokyo Inst. Tech.
----------------	-------------------

Akihiro YOSHIMI	RIKEN
-----------------	-------

Yoshiaki KIYANAGI	Fac. Engineering, Hokkaido Univ.
-------------------	----------------------------------

Takeshi KAWAI	Xi'an Jiaotong Univ.
---------------	----------------------

Haruhiko FUNAHASHI	Osaka Electro-Communication Univ.
--------------------	-----------------------------------

6 Cost Estimation

The proposed experiment needs (1) instruments for the EDM measurement, (2) UCN beam transport, (3) UCN source, (4) proton beam transport from J-PARC LINAC to the UCN source and (5) the construction of building and additional tunnel to accommodate experimental instruments and proton beam transport optics. In this proposal, we list up for (1)-(4).

		(million yen)
building construction		950
proton beam branch and transport	pulse magnet	50
	DC magnets	25
	quadrupoles and power supplies	15
	control	25
	linear part quadrupoles	25
	linear part quadrupoles power supplies	20
	steering magnet	10
	steering magnet power supply	10
	vacuum	25
	beamline radiation shield	15
UCN source	production target	45
	moderator	100
	converter	120
	reflector and radiation shield	150
UCN transport	UCN guide	10
	magnet for rebuncher	20
	power supply for rebuncher magnet	20
	spin flipper	5
	UCN lifter	8
	UCN shutter	8
experimental apparatus	magnetic shield (six-layer)	23
	electrode	5
	high voltage power supply	5
	EDM chamber	10
	coils	10
	stabilized power supply	10
	EDM cell	5
	UCN polarizer and analyzer	3
	UCN detector (^3He)	2
total		1,729

References

- [1] T. Aso *et al.* [J-PARC UCN Taskforce], arXiv:0907.0515 [physics.ins-det].
- [2] F. J. M. Farley *et al.*, Phys. Rev. Lett. **93**, 052001 (2004)
- [3] C. A. Baker *et al.*, Phys. Rev. Lett. **97**, 131801 (2006)
- [4] <http://ucn.web.psi.ch/>
- [5] K. Kirch, private communication.
- [6] W. C. Griffith *et al.*, Phys. Rev. Lett. **102**, 101601 (2009)
- [7] M. Golub and J. M. Pendlebury, Phys. Lett. **53A**, 133 (1975)
- [8] A. Saunders *et al.*, Phys. Lett. B **593**, 55 (2004)
- [9] Y. Masuda *et al.*, Phys. Rev. Lett. **89**, 284801 (2002)
- [10] C.-Y. Liu, A. R. Young, and S. K. Lamoreaux, Phys. Rev. B **62**, 3581 (2000)

- [11] Dissertation of Chen-Yu Liu, "A Superthermal Ultra-Cold Neutron Source", Princeton University, (2002)
- [12] Dissertation of Kenji Mishima, "Irradiation effect of Ortho deuterium for UCN source", Osaka University, (2004)
- [13] F. Atchison *et al.*, Phys. Rev. Lett. **95**, 182502 (2005)
- [14] H. Iwase, K. Niita and T. Nakamura, J. Nucl. Sci. Technol. **39**, 1142 (2002)
- [15] Z-Ch. Yi *et al.*, Condensed Matter **62**, 137 (1986)
- [16] D. Budker *et al.*, Phys. Rev. A **62**, 043403 (2000)
- [17] D. Budker *et al.*, Phys. Rev. A **65**, 055403 (2002)
- [18] T. Oku *et al.*, Physica B **397**, 188 (2007)